A minimalist approach to BL Lacertae: explaining gamma-ray spectral and temporal variability with a single physical parameter

Raniere de Menezes*
Centro Brasileiro de Pesquisas Físicas, 22290-180, Rio de Janeiro, RJ, Brazil

Francesco Massaro and Elisa Visentin
INFN – Istituto Nazionale di Fisica Nucleare, Sezione di Torino, via Pietro Giuria 1, I-10125 Turin, Italy   and
Dipartimento di Fisica, Università degli Studi di Torino, via Pietro Giuria 1, I-10125 Torino, Italy

Federico Di Pierro
INFN – Istituto Nazionale di Fisica Nucleare, Sezione di Torino, via Pietro Giuria 1, I-10125 Turin, Italy

Haocheng Zhang
University of Maryland Baltimore County, Baltimore, MD 21250, USA   and
NASA Goddard Space Flight Center, Greenbelt, MD 20771, USA

(Dated: December 17, 2025)

The eponymous BL Lac object BL Lacertae is one of the most well-monitored active galactic nuclei, frequently observed from radio to gamma rays. Its relatively soft γ-ray spectrum peaks near 500 MeV, and since 2020 it has undergone an exceptional series of flaring episodes. The observed emission is well described by synchrotron self-Compton (SSC) models, with negligible contribution from external seed photons. We investigate the physical origin of BL Lacertae's γ-ray temporal and spectral variability using data from the Large Area Telescope (LAT) on board the *Fermi* Gamma-ray Space Telescope, and show that this variability can be explained by a single varying parameter, namely the electrons' peak energy, γ_p, under a single-zone SSC scenario with a log-parabolic electron distribution. We use a Markov chain Monte Carlo to estimate the spectral parameters of BL Lacertae over time, selected from an adaptive-binned gamma-ray light curve. We then study the correlation between the inverse Compton peak luminosity, L_{IC}, and the position of this peak on the SED energy axis, E_p, and compare it with what is expected for a single-zone SSC scenario when only one parameter is free to vary. We find a correlation $L_{IC} = 10^{42.33\pm0.15\pm0.18_{sys}} E_p^{0.98\pm0.05\pm0.06_{sys}}$, consistent, within the errors, with the linear relation $L_{IC} \propto E_p$, expected when γ_p is the only free parameter in the assumed SSC model. This result supports a minimalist SSC scenario in which changes in γ_p dominate the observed temporal and spectral variability of BL Lacertae.

I. INTRODUCTION

BL Lac objects are characterized by the lack of strong optical–infrared lines [equivalent widths < 5 Å; 1–3], significant variability across the electromagnetic spectrum on time scales from years to minutes [4–6], and a non-thermal spectral energy distribution (SED) with a synchrotron bump peaking between the infrared and X-rays [7] and a high-energy bump in the gamma-ray band [8, 9].

The highly variable gamma-ray emission from BL Lac objects likely originates in a compact region–unresolved by current instruments–located at distances ranging from subparsec scales to a few parsecs from the central black hole [10, 11]. Flaring states usually come with changes in the hardening of the gamma-ray spectrum [12], and understanding how the flux correlates with the spectral hardening can reveal the underlying mechanism behind the observed variability [13].

In this work, we analyze nearly 17 years of *Fermi* Large Area Telescope [LAT; 14] observations to investigate the spectral variability of the eponymous BL Lac object BL Lacertae in gamma rays. Our choice of this target is motivated by the availability of extensive LAT data, allowing the construction of a large sample of high-quality, log-parabolic gamma-ray spectra across different activity states. In the LAT Fourth Source Catalog[15] [4FGL-DR4; 16, 17], BL Lacertae is the second most significant BL Lac object (after Mrk 421), with its spectral peak located near 500 MeV. Mrk 421 is not considered here, as its gamma-ray emission peaks around 100 GeV, requiring joint analyses with imaging atmospheric Cherenkov telescopes (IACTs) to precisely constrain its spectral shape across different activity states. We propose that the temporal and spectral variability of BL Lacertae can be interpreted through a single physical parameter, assuming its gamma-ray emission arises from a one-zone synchrotron self-Compton (SSC) model [18, 19] and that the electron energy distribution follows a log-parabolic form [20–23] $n(\gamma) = n_0 \left(\gamma/\gamma_0\right)^{-s-r\log_{10}(\gamma/\gamma_0)}$, where n_0 is the density of emitters per interval of γ (cm^{-3}), γ_0 is the electrons' turn-over energy, r the spectral curvature, and s the spectral slope. This simplified model has been repeatedly applied to BL Lacertae, consistently providing a good description of the data [24–26].

---
* Contact author: raniere@cbpf.br; Centro Brasileiro de Pesquisas Físicas, 22290-180, Rio de Janeiro, RJ, Brazil
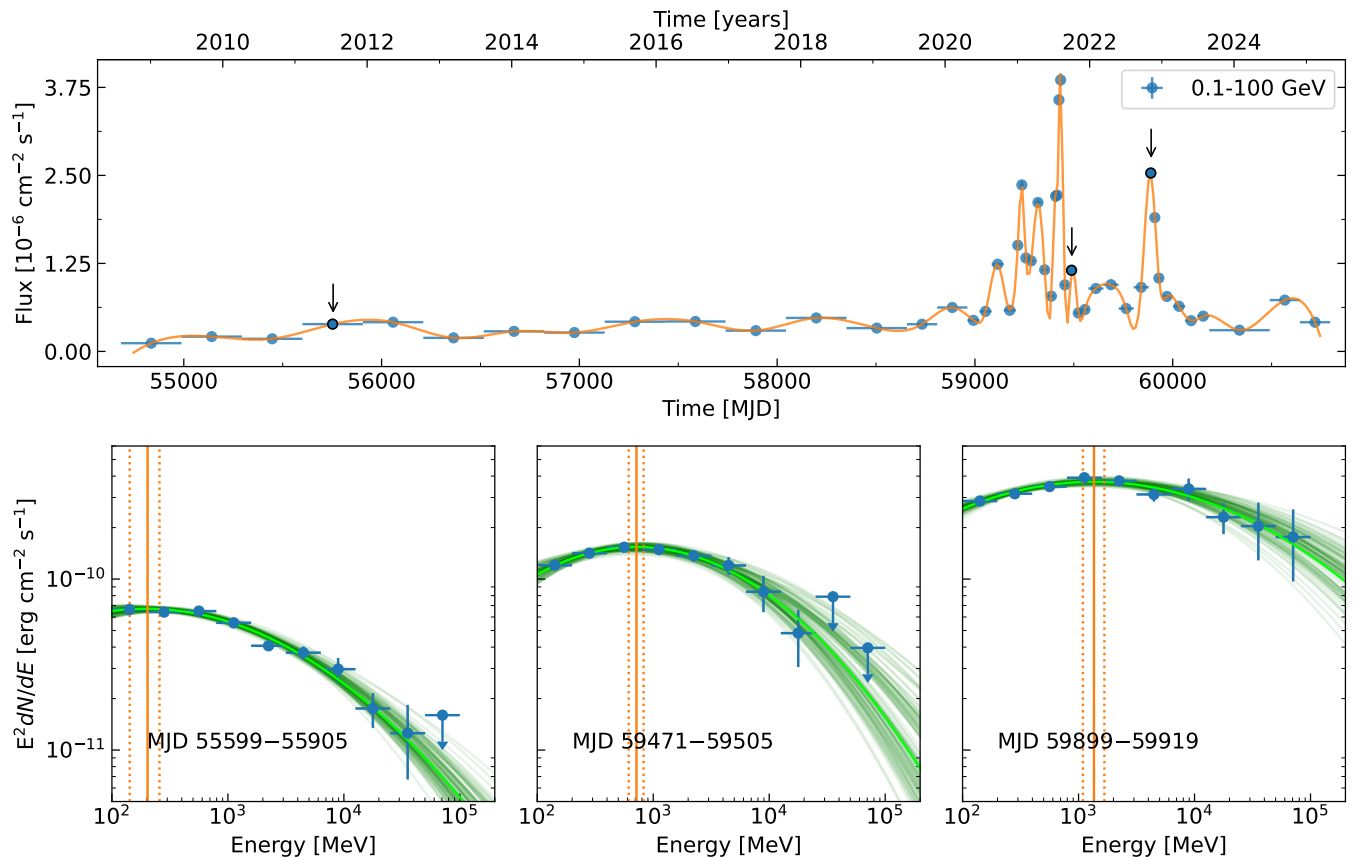
FIG. 1. Temporal (top) and spectral (bottom) evolution of BL Lacertae in gamma rays. In the integrated photon-flux light curve shown in the top panel, the three arrows mark the time bins corresponding to the three spectra shown in the bottom panels. The chosen TS for upper limits is set to 25. In the bottom panels, we can see that the log-parabola (green solid line) maximum likelihood spectral peak (orange vertical line) shifts towards higher energies when the gamma-ray flux increases. The dotted vertical lines represent the 68% containment interval for the MCMC posterior distribution on E_p. The spectra presented here are in the observed frame.

Our main goal is to study how the isotropic inverse Compton (IC) peak luminosity, L_{IC}, evolves with the peak energy in the SED, E_p. If the gamma-ray emission of BL Lacertae is dominated by Thomson scattering [see 13], then $L_{IC} \propto E_p$ when the only varying parameter is the energy at the peak of the electron distribution γ_p (note that $\gamma_p \propto \gamma_0$ when given a fixed r and s, i.e., $\gamma_p = \gamma_0 10^{-s/2r}$)[27], $L_{IC} \propto E_p^2$ when only the magnetic field B varies, and $L_{IC} \propto E_p^4$ when only the beaming factor δ varies. In contrast, if Klein–Nishina effects dominate, the luminosity must scale as $L_{IC} \propto E_p^4$, with δ as the sole varying parameter.

This paper is organized as follows. Section II presents the gamma-ray LAT data selection and analysis. In Section III, we report our findings and show that the spectral variability can be explained by changes in a single SSC parameter, namely the energy at the peak of the electron distribution. In Section IV, we discuss and summarize our results. Throughout this work we adopt $H_0 = 0.70$ km s^{-1} Mpc^{-1}, $\Omega_m = 0.30$, and $\Omega_\Lambda = 0.70$ [28].

II. DATA SELECTION AND ANALYSIS

Our dataset comprises nearly 17 years of *Fermi*-LAT Pass 8 [29] R3 [30] observations, spanning from August 4, 2008, to May 1, 2025 and in the energy range from 0.1 to 100 GeV. The data analysis was performed with `easyfermi`[31] 2.0.18 [32], which is heavily based on `fermipy`[33] 1.4.0 [34] and `fermitools`[35] 2.2.0, by means of a binned likelihood analysis and using NEWMI-NUIT as the minimizer.

The $15° \times 15°$ region of interest (RoI) was centered on BL Lacertae and modeled with all 4FGL-DR4 sources [16, 17] plus additional point-like sources detected above 4σ. The spectral shape and normalization of sources within $7°$ of BL Lacertae were left free to vary during the fit, while those up to $5°$ outside the RoI were fixed in their 4FGL-DR4 values. For each energy decade, we divided the data into eight logarithmic bins, using SOURCE events (evclass = 128) detected in the front or back layers of the tracker (evtype = 3). We applied standard quality cuts (DATA_QUAL > 0, LAT_CONFIG

== 1) and excluded events with zenith angles $\theta_z > 90°$. The Galactic and isotropic backgrounds[36] were modeled with `gll_iem_v07` and `iso_P8R3_SOURCE_V3_v1`, and the normalization of both components was left free to vary. Detection significance was estimated as $\sqrt{TS}$, where $TS = 2(\mathcal{L}_1 - \mathcal{L}_0)$ compares the maximum log-likelihoods with and without the target [37].

We built an adaptive-binning photon flux light curve for BL Lacertae (top panel of Fig. 1) using the `easyfermi` method[38] integrated from 0.1 to 100 GeV, in which we start by building a constant-binning light curve (20 bins in our case) and then further slice the bins with $TS > 2TS_{th}$ into smaller pieces. We set the TS threshold as $TS_{th} = 9000$, which is a good compromise between variability resolution and photon statistics above 10 GeV, necessary to constrain the spectral shape in time intervals where E_p shifts to higher energies. The final light curve has 47 bins, 21 of which do not exceed the TS threshold; however, this does not compromise the analysis since these bins correspond to lower fluxes and lower values of E_p, for which the log-parabolic curvature remains well constrained. The model adopted to build the light curve is the log-parabola available in `fermitools` 2.2.0[39], where we left the normalization, slope, and curvature free to vary.

For each bin in the adaptive-binning light curve, we computed a gamma-ray spectrum with the `fermipy` function `sed()`, corrected them for extragalactic background light absorption with `gammapy` [rather small effect; 40, 41] adopting a redshift $z = 0.0686$ [42], and used a Markov chain Monte Carlo [43] to estimate the parameters of the log-parabolic model [see 21, 44, 45] conveniently defined by

$$S(E) = E^2 dN/dE = S_p 10^{-\beta \log_{10}^2 (E/E_p)}, \qquad (1)$$

where S_p is the differential energy flux at the log-parabola peak in erg cm^{-2} s^{-1}, β is the spectral curvature, and E_p is the position of the log-parabola peak in the energy axis in MeV. This parametrization is convenient since we can directly estimate S_p and E_p, as well as their corresponding errors, without resorting to huge error propagation formulas. The adopted priors span broad ranges so that they remain unchanged across all fits. Specifically, we use a flat prior distribution for $0 < \beta < 1$, and log-flat prior distributions for $100 < E_p < 10^5$ and $10^{-12} < S_p < 10^{-8}$. In the bottom panels of Fig. 1, we show three gamma-ray spectra of BL Lacertae selected at the three light curve bins tagged with arrows in the upper panel. From left to right, they have $TS = 8988, 8111, 12337$, and $E_p = 205^{+50}_{-59}, 724^{+100}_{-100}, 1343^{+275}_{-238}$ MeV, respectively. Here we see that an increase in S_p is followed by an increase in E_p. The dependency of S_p on E_p will reveal the physics causing the spectral variability, as discussed in the next sections.

A. Multiwavelength data

To estimate the parameters for the broadband SED of BL Lacertae, we selected 13 lower energy data points from archival observations using the online SED builder tool[46]. These observations and respective references are listed in Table I in Appendix A. We use these observations in the next section to roughly constrain the single-zone SSC parameters for BL Lacertae. A precise modeling of the SED is not the goal at this point of this work since we are interested only in the evolution of the SED and, in particular, in how S_p grows with E_p. These archival data points range from radio to X-rays, while for the gamma-ray energies, we used the integrated *Fermi*-LAT spectrum for the whole time window of almost 17 years.

III. RESULTS

The evolution of the isotropic SED peak luminosity ($L_{IC} = 4\pi D_L^2 S_p$, with D_L the luminosity distance) as a function of E_p is shown in the top panel of Fig. 2. The orthogonal distance regression (ODR) fit (green line), parameterized as $L_{IC} = 10^{N_0} E_p^\Gamma$, yields $N_0 = 42.33 \pm 0.15$ and $\Gamma = 0.98 \pm 0.05$, consistent within errors (gray lines) with a single-zone SSC model where only γ_p varies. A jackknife resampling (inset) confirms the robustness of this correlation, giving

$$L_{IC} = 10^{42.33 \pm 0.15 \pm 0.18_{\text{sys}}} E_p^{0.98 \pm 0.05 \pm 0.06_{\text{sys}}},$$

where the systematic errors represent the σ of the jackknife parameter distributions. This result is free of bias driven by up to four points in our dataset (representing more than 10% of our sample). We also find a relatively strong Pearson correlation coefficient of $P_c = 0.78$ with a p-value for non-correlation of 5.2×10^{-8}, corresponding to $> 5\sigma$ significance. For comparison, the black dashed lines in Fig. 2 show the expected Thomson-regime scalings for variations in γ_p ($\Gamma = 1$) or B ($\Gamma = 2$), while the red dashed line represents the case where only the beaming factor δ varies, giving $\Gamma = 4$ in both Thomson and Klein–Nishina regimes.

The upper limits in Fig. 2 are defined when $E_p < 300$ MeV or when uncertainties allow E_p values below 100 MeV. Adopting alternative thresholds of 200 MeV or 400 MeV yields $L_{IC} = 10^{42.61 \pm 0.12 \pm 0.14_{\text{sys}}} E_p^{0.90 \pm 0.05 \pm 0.05_{\text{sys}}}$ and $L_{IC} = 10^{42.12 \pm 0.17 \pm 0.14_{\text{sys}}} E_p^{1.06 \pm 0.06 \pm 0.05_{\text{sys}}}$, respectively, both consistent with the linear correlation expected from variations in the electron peak energy.

For a log-parabolic electron distribution, the synchrotron curvature is expected to scale as $b \propto 1/\log(E_p)$ [47]. For the IC peak in the Thomson regime (as suggested for BL Lacertae by the correlation in the top panel of Fig. 2), the curvature β should follow a similar but systematically smaller trend due to energy redistribution in
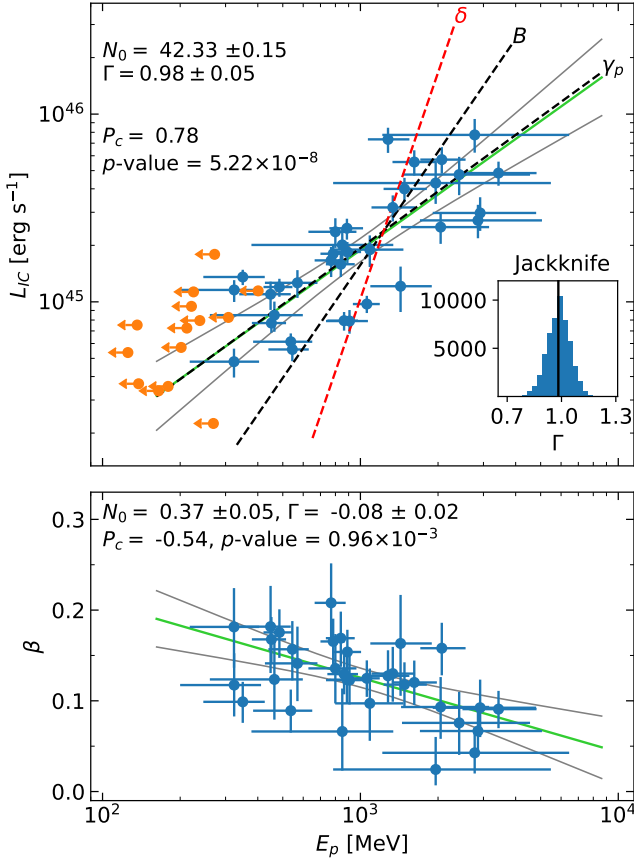
FIG. 2. Rest-frame correlations of L_{IC} and β with E_p. Top: L_{IC} scales nearly linearly with E_p, consistent with variability driven mainly by changes in γ_p. The inset shows the jackknife resampling distribution of the slope, centered at $\Gamma = 0.98$. Orange points mark upper limits on E_p (not included in the fit), defined when $E_p < 300$ MeV or when uncertainties extend below 100 MeV. Dashed lines indicate the correlations expected if variability depends on a single parameter (see text). Bottom: The spectral curvature β shows no significant dependence on E_p, suggesting BL Lacertae may be transitioning out of the Thomson regime. N_0 and Γ are described in the text.

the scattering process [22]. In general, β is expected to anticorrelate with E_p in the Thomson regime, show no correlation in the transition to the Klein–Nishina regime, and become positively correlated in the Klein–Nishina regime [47]. Our data (bottom panel of Fig. 2) shows a weak negative trend, $\beta = (0.37 \pm 0.05)E_p^{-0.08\pm0.02}$, with $P_c = -0.54$ and a p-value $\sim 10^{-2}$. These results suggest BL Lacertae may be entering the hybrid Thomson/Klein–Nishina regime, where no clear β–E_p correlation is expected. This trend also indicates that the highest luminosity SEDs will tend to have smaller curvatures, which are harder to constrain, explaining why some of our data points in Fig. 2 with luminosities above $\sim 3 \times 10^{35}$ erg s^{-1} present relatively large uncertainties in E_p.

A. Precise SED evolution

Assuming a log-parabolic electron distribution (Sect. I) within a single-zone SSC framework, we use JetSeT 1.3.0[48] [47, 49, 50] to study the evolution of BL Lacertae's SED when only the peak electron energy γ_p (or equivalently γ_0, see Sect. I) is allowed to vary. To set up the model, we first fit the archival multiwavelength data described in Sect. II A, and then adopt the rounded parameters of this fit as our starting model (see Fig. 4 and Table II in Appendix A).

With all other parameters fixed, we let γ_p vary from $10^{5.5}$ to 10^9 ($10^3 \lesssim \gamma_0 \lesssim 10^7$). The resulting SED evolution follows the expected trend: linear L_p–E_p scaling in the Thomson regime, steeper growth in the intermediate Thomson/Klein-Nishina regime, and eventual convergence of L_p to a constant at the highest γ_p values (Fig. 3). In that figure, the blue-to-yellow gradient traces IC spectra as γ_p increases, while the green line shows the jackknife correlation derived from our data. The results indicate that BL Lacertae is mostly in the Thomson regime, though during strong flares it approaches the Thomson/Klein-Nishina transition, consistent with the weak β–E_p correlation found earlier [see Fig. 10 in 47, for a detailed discussion on this topic].

IV. DISCUSSION AND CONCLUSIONS

In this work, we argue that the temporal and spectral variability of BL Lacertae in γ rays can be explained mainly by changes in the electron peak energy γ_p in a single-zone SSC scenario. The expected correlation $L_{IC} \propto E_p$ is well reproduced by our result, $L_{IC} = 10^{42.33\pm0.15\pm0.18_{\rm sys}}E_p^{0.98\pm0.05\pm0.06_{\rm sys}}$, which is also in line with previous multiwavelength studies of blazars in different activity states [51–53]. However, the relatively large scatter ($RMS_\perp = 0.19$ in the log space, which is comparable to the average effective orthogonal uncertainties, given by $\langle \sigma_{\perp,i} \rangle = \left\langle \sqrt{(\sigma_{x,i}\sin\theta)^2 + (\sigma_{y,i}\cos\theta)^2} \right\rangle = 0.27$, where $\theta = \arctan(\Gamma)$) shown in Figure 2 opens the possibility for other parameters to play a secondary role in the observed variability. Furthermore, the weak negative (or absent) correlation $\beta = (0.37 \pm 0.05)E_p^{-0.08\pm0.02}$ indicates that BL Lacertae is likely approaching a hybrid Thomson/Klein-Nishina regime [see 54, for a discussion on this topic].

In the Thomson regime, it is also possible to have a correlation of the form $L_{IC} \propto E_p^\Gamma$, with $\Gamma < 1$, and depending only on γ_p. This holds if we make the further assumption that the size of the emitting region, R, depends on the electrons' diffusion coefficient (D) and cooling time scale (τ), $R = \sqrt{D\tau} \propto \gamma^{(\alpha-1)/2}$ [55], where the index α can range from $1/3$ in the Kolmogorov turbulence regime to 1 in the Bohm approximation, and γ is the energy of the electrons, here approximated as $\gamma \approx \gamma_p$, meaning that we assume a roughly mono-energetic elec-
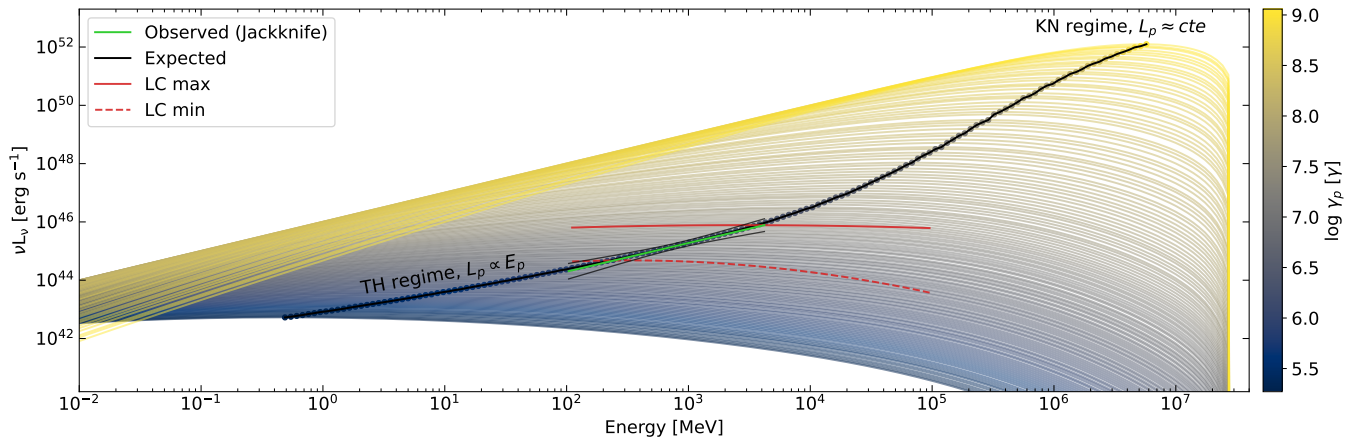
FIG. 3. Evolution of BL Lacertae's SED when only the electron peak energy γ_p (or equivalently γ_0) is free to vary, while all other parameters are fixed to the values in Table II. The black line tracks the IC peak positions, the green line shows the jackknife correlation derived from the data, and the color gradient represents the SSC emission models for different values of γ_p. The results indicate that BL Lacertae remains mostly in the Thomson regime, with hints of entering a Thomson/Klein-Nishina transition during its brightest flares. The red curves correspond to the log-parabolic models fitted to the highest- and lowest-flux bins shown in the light curve of Fig. 1.

tron population. For example, if $\alpha = 1/3$, the expected correlation computed with JetSeT for BL Lacertae in the Thomson regime is $L_{IC} \propto E_p^{0.6}$, while if $\alpha = 0.85$, the expected correlation is $L_{IC} \propto E_p^{0.9}$, as found in our alternative analysis when we set the upper limits threshold at 200 MeV. In this last case, the dependency of R on γ_p is minimal, going as $R \propto \gamma_p^{-0.075}$. Finally, if $\alpha = 1$, we fall exactly in the correlation discussed in the rest of this work (i.e., $L_{IC} \propto E_p$), where the size of the emission region is a constant.

This work required a large amount of high-quality gamma-ray data, enabled by the exceptional brightness of BL Lacertae, the location of its IC peak near 500 MeV, and the uninterrupted all-sky monitoring provided by Fermi-LAT. Other promising candidates for future studies include the BL Lac objects Mrk 421 and S5 0716+71. However, their γ-ray spectra are often better described by a power law with an exponential cutoff (PLEC) rather than a log-parabola, meaning that a parametrization of the PLEC in terms of S_p and E_p, such as the one available in easyfermi[56] [32] may be useful:

$$S(E) = S_p \left(\frac{E_p}{E}\right)^{a-2} e^{((2-a)/b)(1-(E/E_p)^b)}, \quad (2)$$

where a is the power law spectral index, and b is the super-exponential index. Moreover, their IC peaks are located at higher energies, meaning that the usage of IACTs, such as the Large-Sized Telescope [57] or the Cherenkov Telescope Array [58], may be necessary. Extending this analysis to other BL Lacs in the gamma-ray band would yield further insights into their emission mechanisms, particularly if their variability also proves to be primarily governed by the single parameter γ_p.

Freq. (Hz)	Flux (erg cm^{-2} s^{-1})	Reference
4.85×10^9	$(1.43 \pm 0.13) \times 10^{-13}$	[60]
4.40×10^{10}	$(1.87 \pm 0.07) \times 10^{-12}$	[61]
1.43×10^{11}	$(4.19 \pm 0.09) \times 10^{-12}$	[61]
5.00×10^{12}	$(2.01 \pm 0.46) \times 10^{-11}$	[62]
1.67×10^{13}	$(5.32 \pm 0.57) \times 10^{-11}$	[63]
6.52×10^{13}	$(9.47 \pm 0.22) \times 10^{-11}$	[64]
8.56×10^{14}	$(6.82 \pm 0.04) \times 10^{-11}$	[65]
1.69×10^{17}	$(6.49 \pm 2.06) \times 10^{-12}$	[66]
9.63×10^{17}	$(7.14 \pm 0.46) \times 10^{-12}$	[66]
2.30×10^{18}	$(4.32 \pm 1.15) \times 10^{-12}$	[66]
7.35×10^{18}	$(2.27 \pm 1.23) \times 10^{-11}$	[66]
1.31×10^{19}	$(2.16 \pm 1.14) \times 10^{-11}$	[66]
1.76×10^{19}	$(1.69 \pm 1.31) \times 10^{-11}$	[66]
3.09×10^{22}	$(7.79 \pm 0.07) \times 10^{-11}$	This work
5.07×10^{22}	$(8.18 \pm 0.05) \times 10^{-11}$	This work
8.30×10^{22}	$(8.39 \pm 0.07) \times 10^{-11}$	This work
1.36×10^{23}	$(8.46 \pm 0.07) \times 10^{-11}$	This work
2.23×10^{23}	$(8.22 \pm 0.07) \times 10^{-11}$	This work
3.65×10^{23}	$(7.44 \pm 0.06) \times 10^{-11}$	This work
5.97×10^{23}	$(7.17 \pm 0.10) \times 10^{-11}$	This work
9.79×10^{23}	$(6.55 \pm 0.12) \times 10^{-11}$	This work
1.60×10^{24}	$(6.02 \pm 0.10) \times 10^{-11}$	This work
2.62×10^{24}	$(5.43 \pm 0.18) \times 10^{-11}$	This work
4.30×10^{24}	$(4.27 \pm 0.19) \times 10^{-11}$	This work
7.04×10^{24}	$(3.03 \pm 0.20) \times 10^{-11}$	This work
1.15×10^{25}	$(2.34 \pm 0.16) \times 10^{-11}$	This work
1.89×10^{25}	$(1.44 \pm 0.24) \times 10^{-11}$	This work

TABLE I. Multiwavelength archival and new observations of BL Lacertae. The *Fermi*-LAT data listed here correspond to 17 years of observations.

Parameter	Value	Units	Free
Region size, R	2.84×10^{16}	cm	Yes
Magnetic field, B	0.03	G	Yes
Beaming factor, δ	31.36	Lor. factor	Yes
Low-energy cutoff, γ_{min}	81.89	Lor. factor	Yes
High-energy cutoff, γ_{max}	1.92×10^6	Lor. factor	Yes
Density of emitters, n_0	20.0	cm^{-3}	Yes
Turn-over energy, γ_0	4.55×10^3	Lor. factor	Yes
Spectral slope, s	2.6	–	No
Spectral curvature, r	0.58	–	Yes

TABLE II. List of rounded SED parameters for BL Lacertae. The errors are omitted because they are not useful in our analysis.

Appendix A: SED multiwavelength data and parameters

In Table I, we list the multiwavelength archival and new observations used to model the SED of BL Lacertae. The corresponding SSC model rounded parameters are given in Table II, while uncertainties are omitted because we are interested only on approximate values. The spectral slope of the electron distribution was set as $s = 2.6$ for convenience, and has no impact on the results. The data and best-fit model from these tables are shown in Fig. 4.

[1] M. Stickel, P. Padovani, C. Urry, J. Fried, and H. Kühr, The complete sample of 1 jansky bl lacertae objects. i-summary properties, The Astrophysical Journal **374**, 431 (1991).
[2] R. de Menezes, H. A. Peña-Herazo, E. J. Marchesini, R. D'Abrusco, N. Masetti, R. Nemmen, F. Massaro, F. Ricci, M. Landoni, A. Paggi, *et al.*, Optical characterization of wise selected blazar candidates, Astron. Astrophys. **630**, A55 (2019).
[3] R. de Menezes, R. A. Amaya-Almazán, E. J. Marchesini, H. A. Peña-Herazo, F. Massaro, V. Chavushyan, A. Paggi, M. Landoni, N. Masetti, F. Ricci, *et al.*, Optical spectroscopic observations of gamma-ray blazar candidates. x. results from the 2018–2019 soar and oan-spm observations of blazar candidates of uncertain type, Astrophysics and Space Science **365**, 12 (2020).
[4] J. Albert, E. Aliu, H. Anderhub, P. Antoranz, A. Armada, C. Baixeras, J. Barrio, H. Bartko, D. Bastieri, J. Becker, *et al.*, Variable very high energy γ-ray emission from markarian 501, The Astrophysical Journal **669**, 862 (2007).
[5] F. Aharonian, A. Akhperjanian, A. Bazer-Bachi, B. Behera, M. Beilicke, W. Benbow, D. Berge, K. Bernlöhr, C. Boisson, O. Bolz, *et al.*, An exceptional very high energy gamma-ray flare of pks 2155–304, The Astrophysical Journal **664**, L71 (2007).
[6] T. Arlen, T. Aune, M. Beilicke, W. Benbow, A. Bouvier, J. Buckley, V. Bugaev, A. Cesarini, L. Ciupik, M. Connolly, *et al.*, Rapid tev gamma-ray flaring of bl lacertae, The Astrophysical Journal **762**, 92 (2012).
[7] R. de Menezes, R. D'Abrusco, and F. Massaro, The origin of mid-infrared colors in γ-ray blazars, Astron. Astrophys. **695**, A56 (2025), arXiv:2502.03466 [astro-ph.HE].
[8] F. Tavecchio, L. Maraschi, and G. Ghisellini, Constraints on the physical parameters of tev blazars, The Astrophysical Journal **509**, 608 (1998).
[9] M. Böttcher, A. Reimer, K. Sweeney, and A. Prakash, Leptonic and hadronic modeling of fermi-detected blazars, The Astrophysical Journal **768**, 54 (2013).
[10] I. Agudo, A. P. Marscher, S. G. Jorstad, V. M. Larionov, J. L. Gomez, A. Lähteenmäki, P. S. Smith, K. Nilsson, A. C. Readhead, M. F. Aller, *et al.*, On the location of the γ-ray outburst emission in the bl lacertae object ao 0235+ 164 through observations across the electromagnetic spectrum, The Astrophysical Journal Letters **735**, L10 (2011).
[11] M. Böttcher and P. Els, Gamma–gamma absorption in the broad line region radiation fields of gamma-ray blazars, The Astrophysical Journal **821**, 102 (2016).
[12] J. Deng and Y. Jiang, The spectral variation behavior of fermi-lat blazars, The Astrophysical Journal **983**, 128 (2025).
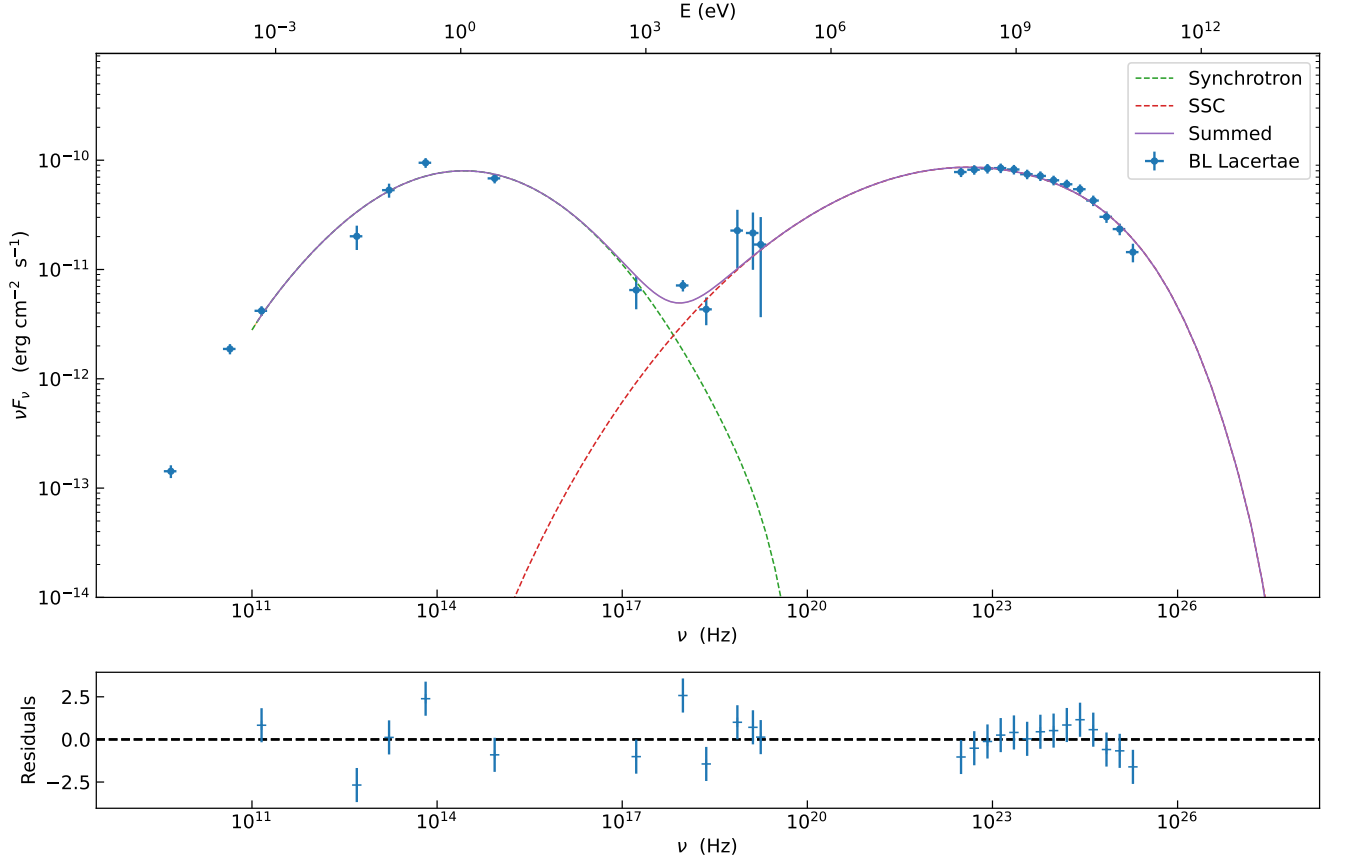
FIG. 4. The best fit one-zone SSC model for the multiwavelength data described in Sect. II A. The rounded parameters for this fit are found in Table II. We use these parameters as a starting point in the investigation of the SED spectral evolution when γ_p (or, equivalently here, γ_0) is the only free variable. The *Fermi*-LAT data shown here covers the 17 years of observations.

[13] F. Massaro, A. Tramacere, A. Cavaliere, M. Perri, and P. Giommi, X-ray spectral evolution of tev bl lacertae objects: eleven years of observations with bepposax, xmm-newton and swift satellites, Astron. Astrophys. **478**, 395 (2008).

[14] W. Atwood, A. A. Abdo, M. Ackermann, W. Althouse, B. Anderson, M. Axelsson, L. Baldini, J. Ballet, D. Band, G. Barbiellini, *et al.*, The large area telescope on the fermi gamma-ray space telescope mission, The Astrophysical Journal **697**, 1071 (2009).

[15] https://fermi.gsfc.nasa.gov/ssc/data/access/lat/14yr_catalog/.

[16] S. Abdollahi, F. Acero, M. Ackermann, M. Ajello, W. Atwood, M. Axelsson, L. Baldini, J. Ballet, G. Barbiellini, D. Bastieri, *et al.*, Fermi large area telescope fourth source catalog, The Astrophysical Journal Supplement Series **247**, 33 (2020).

[17] S. Abdollahi, F. Acero, L. Baldini, J. Ballet, D. Bastieri, R. Bellazzini, B. Berenji, A. Berretta, E. Bissaldi, R. D. Blandford, *et al.*, Incremental fermi large area telescope fourth source catalog, The Astrophysical Journal Supplement Series **260**, 53 (2022).

[18] L. Maraschi, G. Ghisellini, and A. Celotti, A jet model for the gamma-ray emitting blazar 3c 279, Astrophysical Journal, Part 2-Letters (ISSN 0004-637X), vol. 397, no.

1, p. L5-L9. **397**, L5 (1992).

[19] S. D. Bloom and A. P. Marscher, An analysis of the synchrotron self-compton model for the multi–wave band spectra of blazars, Astrophysical Journal v. 461, p. 657 **461**, 657 (1996).

[20] E. Massaro, M. Perri, P. Giommi, and R. Nesci, Log-parabolic spectra and particle acceleration in the bl lac object mkn 421: Spectral analysis of the complete bepposax wide band x-ray data set, Astron. Astrophys. **413**, 489 (2004).

[21] E. Massaro, M. Perri, P. Giommi, R. Nesci, and F. Verrecchia, Log-parabolic spectra and particle acceleration in blazars-ii. the bepposax wide band x-ray spectra of mkn 501, Astron. Astrophys. **422**, 103 (2004).

[22] E. Massaro, A. Tramacere, M. Perri, P. Giommi, and G. Tosti, Log-parabolic spectra and particle acceleration in blazars-iii. ssc emission in the tev band from mkn 501, Astron. Astrophys. **448**, 861 (2006).

[23] C. D. Dermer, D. Yan, L. Zhang, J. D. Finke, and B. Lott, Near-equipartition jets with log-parabola electron energy distribution and the blazar spectral-index diagrams, The Astrophysical Journal **809**, 174 (2015).

[24] M. Ravasio, G. Tagliaferri, G. Ghisellini, P. Giommi, R. Nesci, E. Massaro, L. Chiappetti, A. Celotti, L. Costamante, L. Maraschi, *et al.*, Bl lacertae: Complex spectral

variability and rapid synchrotron flare detected with bepposax, Astron. Astrophys. **383**, 763 (2002).

[25] M. Ravasio, G. Tagliaferri, G. Ghisellini, F. Tavecchio, M. Böttcher, and M. Sikora, Bepposax and multiwavelength observations of bl lacertae in 2000, Astron. Astrophys. **408**, 479 (2003).

[26] A. Abdo, M. Ackermann, M. Ajello, E. Antolini, L. Baldini, J. Ballet, G. Barbiellini, D. Bastieri, K. Bechtol, R. Bellazzini, *et al.*, The first fermi multifrequency campaign on bl lacertae: characterizing the low-activity state of the eponymous blazar, The Astrophysical Journal **730**, 101 (2011).

[27] We can also write γ_p in terms of the peak of the $\gamma^3 n(\gamma)$ distribution $\gamma_{3p} = \gamma_p 10^{-3/2r}$, which is frequently used in blazar literature [see, e.g., Sect. 4.2 in 47].

[28] M. Tegmark, M. A. Strauss, M. R. Blanton, K. Abazajian, S. Dodelson, H. Sandvik, X. Wang, D. H. Weinberg, I. Zehavi, N. A. Bahcall, *et al.*, Cosmological parameters from sdss and wmap, Physical Review D **69**, 103501 (2004).

[29] W. Atwood, A. Albert, L. Baldini, M. Tinivella, J. Bregeon, M. Pesce-Rollins, C. Sgrò, P. Bruel, E. Charles, A. Drlica-Wagner, A. Franckowiak, T. Jogler, L. Rochester, T. Usher, M. Wood, J. Cohen-Tanugi, and S. Zimmer, Pass 8: Toward the Full Realization of the Fermi-LAT Scientific Potential, arXiv e-prints , arXiv:1303.3514 (2013), arXiv:1303.3514 [astro-ph.IM].

[30] P. Bruel, T. H. Burnett, S. W. Digel, G. Johannesson, N. Omodei, and M. Wood, Fermi-LAT improved Pass~8 event selection, arXiv e-prints , arXiv:1810.11394 (2018), arXiv:1810.11394 [astro-ph.IM].

[31] `https://github.com/ranieremenezes/easyFermi`.

[32] R. de Menezes, easyfermi: A graphical interface for performing fermi-lat data analyses, Astronomy and Computing **40**, 100609 (2022).

[33] `https://fermipy.readthedocs.io/en/latest/index.html`.

[34] M. Wood, R. Caputo, E. Charles, M. Di Mauro, J. Magill, J. S. Perkins, and Fermi-LAT Collaboration, Fermipy: An open-source Python package for analysis of Fermi-LAT Data, in *35th International Cosmic Ray Conference (ICRC2017)*, International Cosmic Ray Conference, Vol. 301 (2017) p. 824, arXiv:1707.09551 [astro-ph.IM].

[35] `https://fermi.gsfc.nasa.gov/ssc/data/analysis/software/`.

[36] `https://fermi.gsfc.nasa.gov/ssc/data/access/lat/BackgroundModels.html`.

[37] J. R. Mattox, D. L. Bertsch, J. Chiang, B. L. Dingus, S. W. Digel, J. A. Esposito, J. M. Fierro, R. C. Hartman, S. D. Hunter, G. Kanbach, D. A. Kniffen, Y. C. Lin, D. J. Macomb, H. A. Mayer-Hasselwander, P. F. Michelson, C. von Montigny, R. Mukherjee, P. L. Nolan, P. V. Ramanamurthy, E. Schneid, P. Sreekumar, D. J. Thompson, and T. D. Willis, The Likelihood Analysis of EGRET Data, Astrophys. J. **461**, 396 (1996).

[38] `https://easyfermi.readthedocs.io/en/latest/lightcurve.html`.

[39] `https://fermi.gsfc.nasa.gov/ssc/data/analysis/scitools/source_models.html`.

[40] A. Saldana-Lopez, A. Domínguez, P. G. Pérez-González, J. Finke, M. Ajello, J. R. Primack, V. S. Paliya, and A. Desai, An observational determination of the evolving extragalactic background light from the multiwavelength hst/candels survey in the fermi and cta era, Monthly Notices of the Royal Astronomical Society **507**, 5144 (2021).

[41] A. Donath, R. Terrier, Q. Remy, A. Sinha, C. Nigro, F. Pintore, B. Khélifi, L. Olivera-Nieto, J. E. Ruiz, K. Brügge, *et al.*, Gammapy: A python package for gamma-ray astronomy, Astron. Astrophys. **678**, A157 (2023).

[42] E. Massaro, A. Maselli, C. Leto, P. Marchegiani, M. Perri, P. Giommi, and S. Piranomonte, The 5th edition of the roma-bzcat. a short presentation, Astrophysics and Space Science **357**, 75 (2015).

[43] D. Foreman-Mackey, D. W. Hogg, D. Lang, and J. Goodman, emcee: The MCMC Hammer, Pub. of the Astr. Soc. of the Pac. **125**, 306 (2013), arXiv:1202.3665 [astro-ph.IM].

[44] C. Tanihata, J. Kataoka, T. Takahashi, and G. M. Madejski, Evolution of the synchrotron spectrum in markarian 421 during the 1998 campaign, The Astrophysical Journal **601**, 759 (2004).

[45] A. Tramacere, F. Massaro, and A. Cavaliere, Signatures of synchrotron emission and of electron acceleration in the x-ray spectra of mrk 421, Astron. Astrophys. **466**, 521 (2007).

[46] `https://tools.ssdc.asi.it/`.

[47] A. Tramacere, E. Massaro, and A. M. Taylor, Stochastic Acceleration and the Evolution of Spectral Distributions in Synchro-Self-Compton Sources: A Self-consistent Modeling of Blazars' Flares, Astrophys. J. **739**, 66 (2011), arXiv:1107.1879 [astro-ph.HE].

[48] `https://jetset.readthedocs.io/en/1.2.1.post2/index.html`.

[49] A. Tramacere, P. Giommi, M. Perri, F. Verrecchia, and G. Tosti, Swift observations of the very intense flaring activity of Mrk 421 during 2006. I. Phenomenological picture of electron acceleration and predictions for MeV/GeV emission, Astron. Astrophys. **501**, 879 (2009), arXiv:0901.4124 [astro-ph.HE].

[50] A. Tramacere, JetSeT: Numerical modeling and SED fitting tool for relativistic jets, Astrophysics Source Code Library, record ascl:2009.001 (2020).

[51] F. D'Ammando, E. Antolini, G. Tosti, J. Finke, S. Ciprini, S. Larsson, M. Ajello, S. Covino, D. Gasparrini, M. Gurwell, *et al.*, Long-term monitoring of pks 0537- 441 with fermi–lat and multiwavelength observations, Monthly Notices of the Royal Astronomical Society **431**, 2481 (2013).

[52] M. S. Dutka, R. Ojha, K. Pottschmidt, J. D. Finke, J. Stevens, P. G. Edwards, J. Blanchard, J. E. Lovell, R. Nesci, M. Kadler, *et al.*, Multi-wavelength observations of pks 2142- 75 during active and quiescent gamma-ray states, The Astrophysical Journal **779**, 174 (2013).

[53] M. S. Dutka, B. D. Carpenter, R. Ojha, J. D. Finke, F. D'Ammando, M. Kadler, P. G. Edwards, J. Stevens, E. Torresi, P. Grandi, *et al.*, Multiband observations of the quasar pks 2326–502 during active and quiescent gamma-ray states in 2010–2012, The Astrophysical Journal **835**, 182 (2017).

[54] J. P. van den Berg, M. Böttcher, A. Domínguez, and M. López-Moya, Systematic Physical Characterization of the γ-Ray Spectra of 2FHL Blazars, Astrophys. J. **874**, 47 (2019), arXiv:1901.03494 [astro-ph.HE].

[55] H. Zhang, M. Böttcher, and I. Liodakis, Revisiting high-energy polarization from leptonic and hadronic blazar scenarios, The Astrophysical Journal **967**, 93 (2024).

[56] https://easyfermi.readthedocs.io/en/latest/SED.html.

[57] H. Abe, K. Abe, S. Abe, A. Aguasca-Cabot, I. Agudo, N. A. Crespo, L. Antonelli, C. Aramo, A. Arbet-Engels, C. Arcaro, *et al.*, Observations of the crab nebula and pulsar with the large-sized telescope prototype of the cherenkov telescope array, The Astrophysical Journal **956**, 80 (2023).

[58] K. Bernlöhr, A. Barnacka, Y. Becherini, O. B. Bigas, E. Carmona, P. Colin, G. Decerprit, F. Di Pierro, F. Dubois, C. Farnier, *et al.*, Monte carlo design studies for the cherenkov telescope array, Astroparticle Physics **43**, 171 (2013).

[59] https://tools.ssdc.asi.it/.

[60] P. Gregory, W. Scott, K. Douglas, and J. Condon, The gb6 catalog of radio sources, Astrophysical Journal Supplement v. 103, p. 427 **103**, 427 (1996).

[61] P. A. Ade, N. Aghanim, M. Arnaud, M. Ashdown, J. Aumont, C. Baccigalupi, A. Balbi, A. Banday, R. Barreiro, J. Bartlett, *et al.*, Planck early results. vii. the early release compact source catalogue, Astron. Astrophys. **536**, A7 (2011).

[62] L. Wang and M. Rowan-Robinson, The imperial iras-fsc redshift catalogue, Monthly Notices of the Royal Astronomical Society **398**, 109 (2009).

[63] D. Ishihara, T. Onaka, H. Kataza, A. Salama, C. Alfageme, A. Cassatella, N. Cox, P. Garcia-Lario, C. Stephenson, M. Cohen, *et al.*, The akari/irc mid-infrared all-sky survey, Astron. Astrophys. **514**, A1 (2010).

[64] R. e. Cutri, E. Wright, T. Conrow, J. Fowler, P. Eisenhardt, C. Grillmair, J. Kirkpatrick, F. Masci, H. McCallon, S. Wheelock, *et al.*, Vizier online data catalog: Allwise data release (cutri+ 2013), VizieR Online Data Catalog **2328**, II (2021).

[65] V. Yershov, Serendipitous uv source catalogues for 10 years of xmm and 5 years of swift, Astrophysics and Space Science **354**, 97 (2014).

[66] P. Giommi, M. Capalbi, M. Fiocchi, E. Memola, M. Perri, S. Piranomonte, S. Rebecchi, and E. Massaro, A Catalog of 157 X-ray Spectra and 84 Spectral Energy Distributions of Blazars Observed with BeppoSAX, in *Blazar Astrophysics with BeppoSAX and Other Observatories*, edited by P. Giommi, E. Massaro, and G. Palumbo (2002) p. 63, arXiv:astro-ph/0209596 [astro-ph].